Microtubule Dynamics in Interphase Cells

Eric Schulze and Marc Kirschner

Department of Biochemistry, University of California, San Francisco, California 94143

Abstract. The sites of microtubule growth and the kinetics of elongation have been studied in vivo by microinjection of biotin-labeled tubulin and subsequent visualization with immunocytochemical probes. Immunofluorescence and immunoelectron microscopy demonstrate that injected biotin-labeled subunits are incorporated into new segments of growth which are contiguous with unlabeled microtubules. Rapid incorporation occurs by elongation of existing microtubules and new nucleation off the centrosome. The growth rate is 3.6 μm/min and is independent of the concentration of injected labeled tubulin. This rate of incorporation together with turnover of existing microtubules leads to ~80% exchange in 15 min. The observed kinetics and pattern of microtubule turnover allow for an evaluation of the relevance of several in vitro models for steady-state dynamics to the in vivo situation. We have also observed a substantial population of quasi-stable microtubules that does not exchange subunits as rapidly as the majority of microtubules and may have specialized functions in the cell.

A N understanding of cellular morphogenesis is likely to depend on an understanding of the arrangement of the extensive arrays of fibrous elements collectively termed the cytoskeleton. A prominent component of the cytoskeleton is the microtubule network. Many studies using pharmacological and histological techniques suggest that microtubules play an essential role in cellular morphogenesis (Inoué, 1982). It is known that portions of the cell (neurites, for example) change shape rapidly during cell movement and during the extension of cellular processes (Albrecht-Buehler, 1976; Bray, 1973), but these light microscopic observations do not reveal the changes which are occurring on the molecular level. There is therefore a large gap between observations of cellular morphology and descriptions of the underlying molecular changes. In mitosis, the favorable geometry and density of microtubules in the spindle has allowed observations of living cells to be projected to some extent to the level of molecular detail (Inoué and Ritter, 1975). It is clear from these observations that tubulin subunits must exchange rapidly into the microtubules of the mitotic spindle and that the spindle can react quickly to changing conditions by reversibly altering its shape and mass (Inoué and Sato, 1967). We would like to know whether such dynamic changes also occur during interphase and, if so, for what purpose and by what mechanisms.

Recently, techniques have been developed that could in principle give information about the molecular dynamics of microtubules in living cells and hence information about the mechanism of microtubule assembly. By injection of fluorescently labeled tubulin or by photobleaching labeled microtubules, it was shown that interphase microtubules exchange subunits rapidly (15–20 min), though not as rapidly as the mitotic spindle (Salmon et al., 1984 a, b; Saxton et al., 1984). Though these techniques suggested rapid exchange into the

polymer, they did not have sufficient spatial resolution to show where the subunits were inserted or indeed whether the subunits actually became part of the microtubules. In particular, no spatial asymmetry was detected in the recovery from photobleaching so subunit insertion along the polymer length or adventitious binding of tubulin to microtubules could not be ruled out. Recently, Soltys and Borisy (1985) demonstrated that fluorescein-labeled tubulin injected into cells added to the ends of microtubules in vivo. To evaluate if end addition was consistent with the rapid, almost complete exchange implied by the photobleaching studies, it was necessary to determine the rate and sites of subunit addition in vivo.

The rapidity of the exchange observed by Salmon et al. (1984 a, b) was surprising and posed challenges to many potential models for subunit dynamics in vivo. Several detailed models for subunit/polymer exchange have been provided by in vitro experiments. Early studies of microtubule assembly stressed the similarities between microtubules and simple equilibrium processes (Oosawa and Asakura, 1975). Later, the role of nucleotide hydrolysis was explored experimentally and theoretically with suggestions that microtubules may show treadmilling at steady state (Cote and Borisy, 1981; Hill and Kirschner, 1982; Kirschner, 1980; Margolis and Wilson, 1978). Most recently an unusual form of dynamics has been presented in vitro where growing and shrinking populations of microtubules co-exist at steady state (Hill and Carlier, 1983; Kristofferson et al., 1986; Mitchison and Kirschner, 1984 b; Chen and Hill, 1983). It was suggested that the growing phase has subunit-bound GTP at the ends of the polymer whereas the shrinking phase has subunit-bound GDP at the ends. This condition is termed "dynamic instability."

To address these questions of microtubule dynamics in vivo and the relationship of in vitro to in vivo dynamics, we have injected tubulin labeled with biotin and followed the kinetics

of incorporation with fluorescent and colloidal gold probes. By varying the concentrations of injected tubulin we have also tried to address the question of possible perturbation of the in vivo steady state.

Materials and Methods

Materials

N-Hydroxysuccinimidyl biotin was from Polysciences, Inc. (Warrington, PA); rabbit anti-biotin antibody was from Enzo Biochem, Inc. (New York, NY); and 5-nm colloidal gold–labeled goat anti-rabbit was from Janssen Pharmaceuticals (Beerse, Belgium). Mouse monoclonal anti-β-tubulin was a kind gift of Dr. S. H. Blose (Protein Databases, Inc., Huntington Station, NY). Rhodamine- and fluorescein-conjugated secondary antibodies were from Cappel Laboratories (Cooper Biomedical, Inc., Malvern, PA).

Tubulin Preparation

Phosphocellulose-purified tubulin was prepared from bovine brains by a modification of the procedure of Weingarten et al. (1975) as described in Mitchison and Kirschner (1984a). Protein concentrations were determined by the method of Bradford (1976), using bovine serum albumin as a standard.

Preparation of Biotinylated Tubulin

Biotinylated tubulin was prepared as described in Kristofferson et al. (1986) and Mitchison and Kirschner (1985a) except that the final pellet was resuspended in microinjection buffer (50 mM potassium glutamate, 1 mM MgCl$_2$, pH 6.8). The resuspended tubulin was given a final cold spin as described, frozen in aliquots in liquid nitrogen, and stored at −80°C until use.

Cell Culture

African Green monkey kidney fibroblasts (BSC1) (a kind gift of U. Euteneuer, University of California at Berkeley) were grown in Dulbecco's modified Eagle's medium supplemented with 10% fetal calf serum (Gibco, Grand Island, NY). For microinjection studies, the cells were trypsinized off tissue culture dishes, replated onto 1-in-diameter poly-D-lysine–coated coverslips, and allowed to settle for 1 d.

Microinjection

Cells on coverglasses were placed in a microinjection chamber (10-cm-square, ¼-in-thick, aluminum block with 4 inset ⅛-in ID copper tubes through which warm water was pumped thereby keeping the chamber at 37 ± 0.5°C). The chamber (with the cells facing up and covered with ≈1.5 ml Hepes-buffered Dulbecco's modified Eagle's medium) was then placed on a Nikon Diaphot inverted microscope allowing direct access to the cells from above. The cells were then pressure microinjected using the technique of Graessman and Graessman (1976). Microinjection needles were drawn out to ≈0.5–1.0-μm diameter using a Kopf micropipette puller model 700C (Tujunga, CA). We estimate that ~¹⁄₁₀ of a cell volume was typically injected (Graessmann et al., 1980). During microinjection, the cells were videotaped in real time on a Panasonic time lapse video tape recorder Model NV8030 using an RCA TC1005 video camera (Lancaster, PA).

Immunofluorescence

Cells were prepared for immunofluorescence as described in Drubin et al. (1986). Briefly, cells were washed in PBS for ≈2 s, then immersed 10 min in a permeabilization/fix solution (80 mM Pipes, 5 mM EGTA, 1 mM MGCl$_2$, 1% Empigen [Albright & Wilson, Whitehaven, Cumbria, UK], and 0.3% glutaraldehyde at room temperature. After fixation, the cells were placed in phosphate-buffered saline (PBS) with 1 mg/ml NaBH$_4$ for 7 min to quench the glutaraldehyde. Cells were then washed with a solution of PBS plus 1% Triton X-100 (antibody buffer). For double-label immunofluorescence, successive incubations with antibodies were then carried out. With cells injected with >3 mg/ml biotin-labeled tubulin, the procedure was to incubate successively with rabbit anti-biotin (diluted 1:100 in antibody buffer), rhodamine-conjugated goat anti-rabbit (1:50), mouse monoclonal anti-β-tubulin (1:250), fluorescein-conjugated goat anti-mouse (1:50), and fluorescein-conjugated rabbit anti-goat (1:50) for 15 min each, followed each time by washes with antibody buffer.

For cells injected with <3.0 mg/ml biotin-labeled tubulin, the procedure was the same except that a tertiary rhodamine-labeled rabbit anti-goat antibody (1:50) was used to amplify the biotin–tubulin signal. Finally, the coverslips

were rinsed with antibody buffer, and mounted in 90% vol/vol glycerol, 20 mM Tris, pH 7.9. Microtubules were photographed on hypersensitized Kodak Tech-Pan (2415) film. Hypersensitization was carried out in a Lumicon Model 1200 hypersensitization chamber (Livermore, CA). For the rhodamine and fluorescein filters in a Zeiss Photomicroscope the film speed setting was Din 33, and 27 respectively. The film was developed in Kodak D-19 for 4 min.

Length Measurements

Negatives of microinjected cells were projected onto a GITCO (Rockville, MD) digitizing pad, and all unambiguous microtubule segment lengths (≈200/cell) within the cell were then digitized and stored on an IBM PC for subsequent statistical analysis.

Axoneme Experiments

Axoneme microtubule growth experiments were performed as in Kristofferson et al. (1986). Visualization was by immunofluorescence using mouse anti-tubulin and rhodamine-conjugated goat anti-mouse as described above.

Immunoelectron Microscopy

For immunoelectron microscopy, cells were grown on glow-discharged, poly-D-lysine–coated mylar, and injected as described above. Osmication, block staining, embedding, and sectioning were then performed (Mitchison, T., L. Evans, E. Schulze, and M. Kirschner, manuscript in preparation).

Results

Assembly of Biotin-labeled Tubulin In Vitro

We have shown recently that tubulin labeled with 2 to 3 biotins per tubulin dimer will assemble to give morphologically normal microtubules under the usual in vitro assembly conditions (Mitchison and Kirschner, 1985a). The detailed kinetic properties of biotin–tubulin depend on the molar ratio of modified subunits to unmodified subunits and the exact conditions of the reaction mixture. For example, in 4 M glycerol the on rate at the plus end for the 1:1 mixture of biotin-labeled to unlabeled tubulin was virtually identical to that with unmodified tubulin, whereas in Pipes buffer without glycerol it was inhibited 32% (Kristofferson et al., 1986). In the in vivo experiments presented in this paper, we estimate that the molar ratios of modified to unmodified tubulin produced in the cell after microinjection are in the range of 1:2 to 1:40. At the lower end of this range, we might expect considerably less inhibition. To estimate the inhibition of lower molar ratios we have examined the rate of elongation of tubulin from the plus and minus ends of axonemes at a molar ratio of 1:19 biotin–tubulin to unmodified tubulin. As reported previously (Kristofferson et al., 1986), at a 1:1 molar ratio the growth at the plus and minus ends was inhibited 35 and 58%, respectively (Table I). However, as shown in Table

Table I. Growth Rates Off Axonemes* of Varying Molar Ratios of Tubulin and Biotin–Tubulin

Molar Ratio Biotin–Tubulin/tubulin	(+) end (μm/min)[‡]	(−) end (μm/min)
0:1	0.93 ± 0.03	0.25 ± 0.02
1:1[§]	0.68	0.11
1:19	0.86 ± 0.03	0.23 ± 0.02

* All axoneme regrowth experiments were carried out at tubulin concentrations of 1.7 mg/ml in 80 mM Pipes, 1.0 mM MgCl$_2$, 1.0 mM EGTA, pH 6.8. The protocol is detailed in Kristofferson et al. (1986).

[‡] One microtubule end grows three to four times faster than the opposite end. The faster growing end is defined as the plus end. The minus end is defined as the slower growing end. The indicated errors are ± the SEM (s/√n).

[§] Data from Kristofferson et al. (1986).
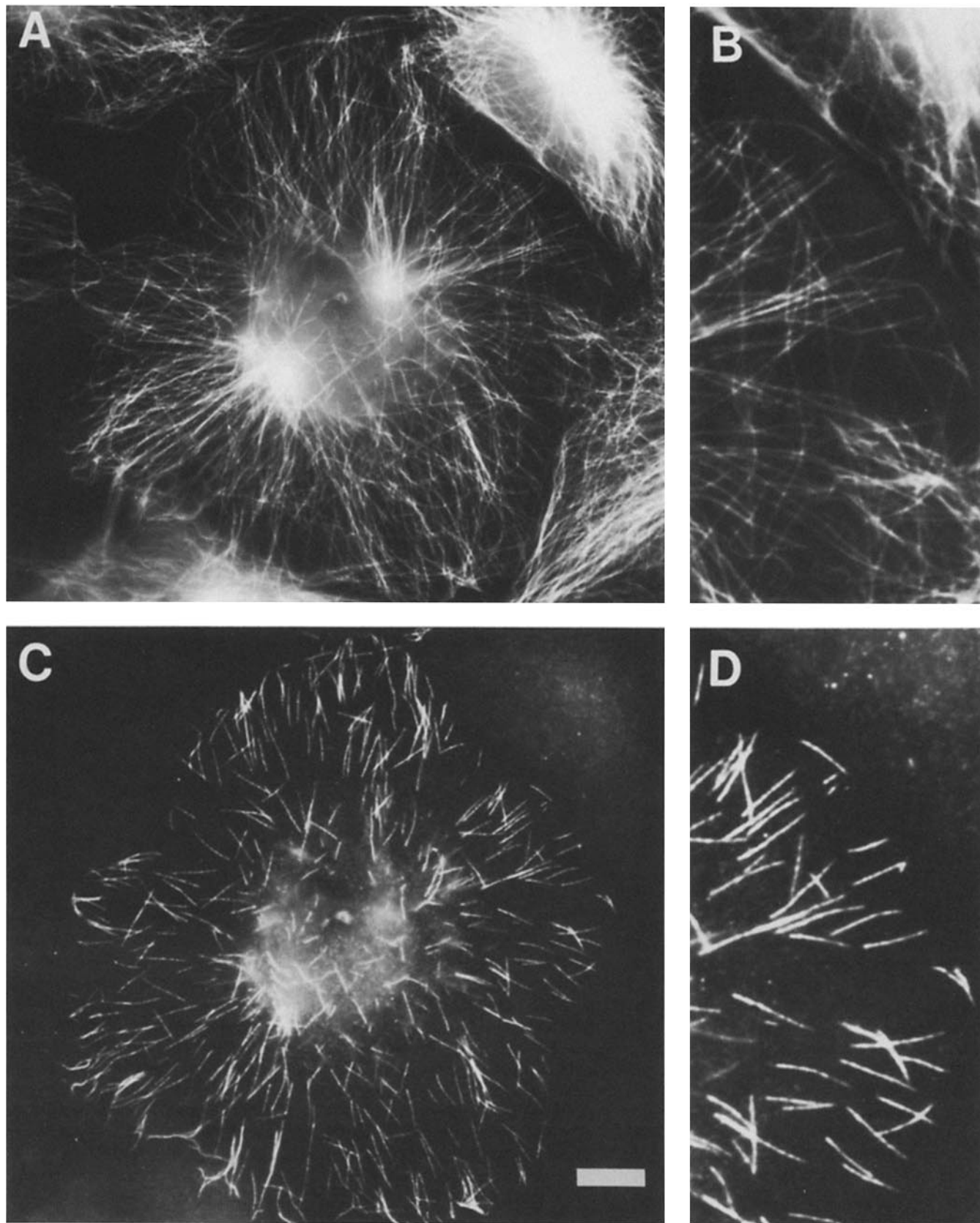
Figure 1. Double-label immunofluorescence of BSC1 fibroblasts showing biotin-labeled microtubule segments at the ends of the microtubules 50 s after injection with biotin–tubulin. (*A*) Fluorescein anti-tubulin staining showing total microtubule network. (*B*) High magnification (2×) view of cell edge showing microtubule ends. (*C*) Rhodamine anti-biotin immunofluorescence showing incorporation of biotin–tubulin. (*D*) High magnification (2×) view of anti-biotin staining, same area as in *B*. By superposition note the staining is at microtubule ends. Bar, 10 μm.

I, at a 1:19 molar ratio, the growth rates at either end were essentially the same as unmodified tubulin.

Microtubules In Vivo Elongate Primarily by Polymerization Off of Pre-existing Microtubule Ends

Cells fixed shortly after injection of biotin-labeled tubulin have incorporated labeled subunits into short segments (Fig. 1 C [50 s after injection]). By comparing the total immunofluorescence pattern (Fig. 1 A) with that of the biotin–tubulin in regions of the cell where microtubule ends can be easily identified, the segments can be shown to be at the ends of microtubules. In the thin region of the cell in Fig. 1 B for example, many microtubule ends can be identified clearly by immunofluorescence of total microtubules. By biotin labeling (Fig. 1 D) most of these ends have incorporated newly polymerized segments. There are of course many more labeled segments in the cell than can be unambiguously assigned to ends visualized by total tubulin immunofluorescence. These segments are in regions of the cell where microtubule density and overlap make visualization of ends difficult. However, in these regions the labeled segments are generally oriented in the same direction as the majority of microtubules, consistent with incorporation of biotin–tubulin onto existing microtubules. We have never seen a random distribution of segments, suggesting spontaneous polymerization as is seen, for example, after recovery from nocodazole (De Brabander et al., 1981).

## The Contiguity of Labeled and Unlabeled Microtubule Segments As Seen by Electron Microscopy

After microinjection, microtubules were visualized by immunoelectron microscopy of thin sections using a rabbit anti-biotin antibody and a goat anti-rabbit antibody labeled with 5-nm colloidal gold. As shown in Fig. 2, microtubules can be found which are labeled evenly with colloidal gold along part of their length. Many such images of contiguous labeled and unlabeled microtubules can be seen in all regions of the cells. The juncture is always very sharp and no evidence is seen for incorporation of biotin-labeled subunits at lower density along essentially unlabeled microtubules.

New Initiation of Microtubules Off Centrosomes

In addition to microtubules apparently growing by elongation, new microtubules seemed to grow from the region of the centrosome. Fig. 3 C shows the anti-tubulin staining of the total microtubule array of a cell injected 66 s before permeabilization and fixation. The centrosome (arrow) can be readily identified as the point of confluence of radially arrayed microtubules. In Fig. 3 D, the antibiotin staining reveals discrete staining of some of these microtubules. Several of the labeled segments seem to emanate directly from the centrosome although at this resolution we could not confirm that these microtubules are a result of direct nucleation. When similar
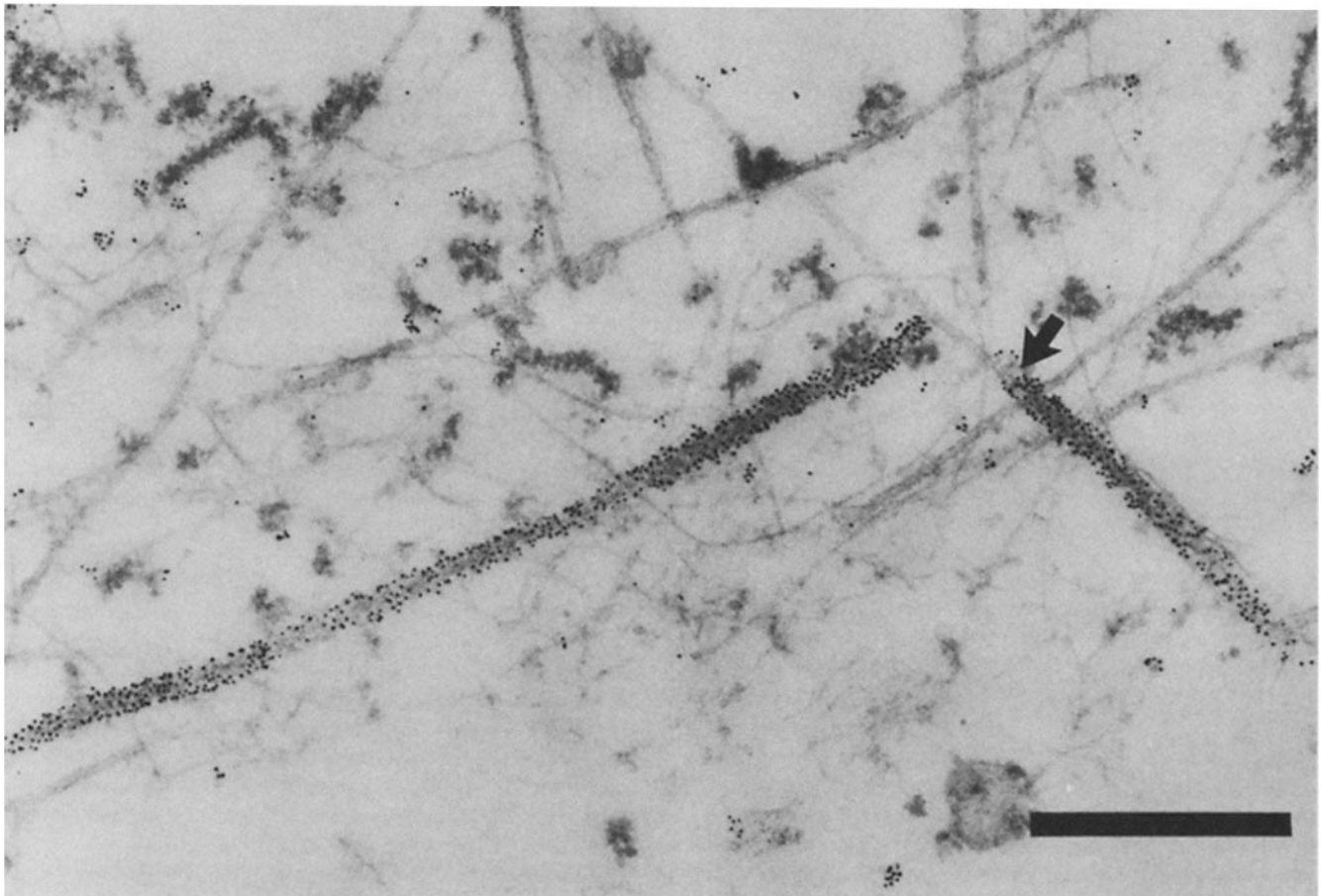

Figure 2. Electron micrograph of interphase BSC1 cell injected 3 min before fixation and stained with 5-nm colloidal gold anti-biotin. Arrow points to junction between labeled and unlabeled segments of a microtubule. Both labeled and unlabeled microtubules can be seen moving in and out of the plane of section without revealing junctions. Bar, 0.5 μm.
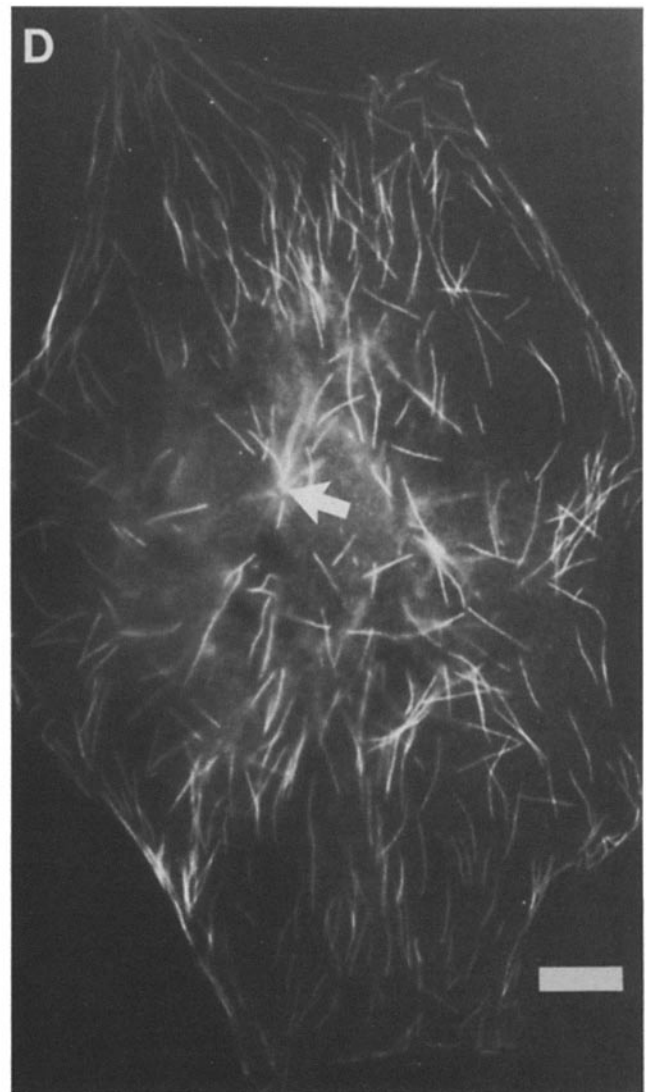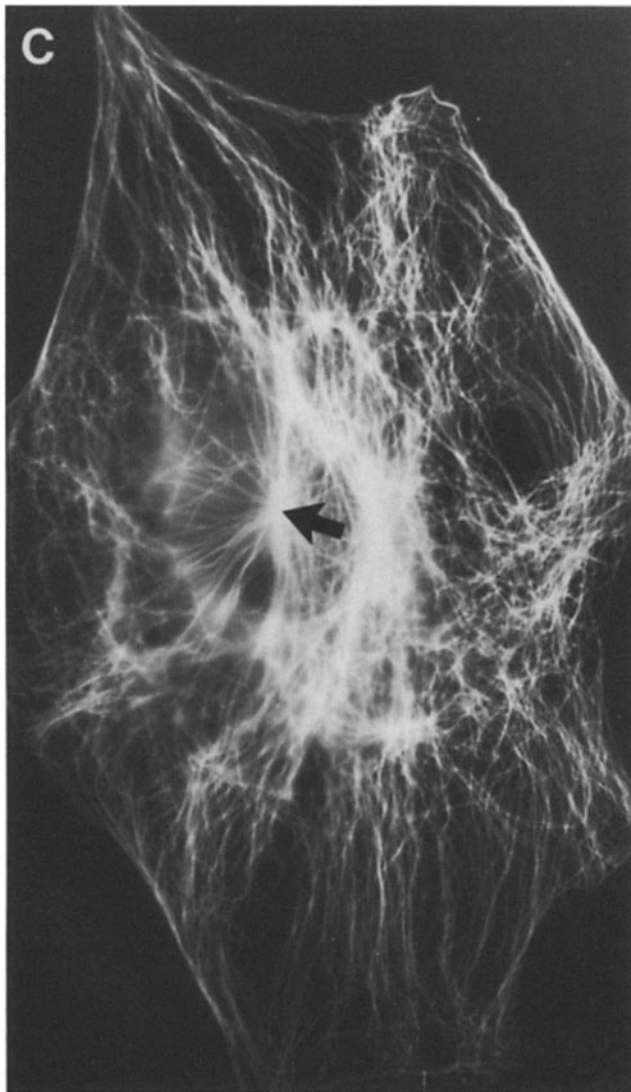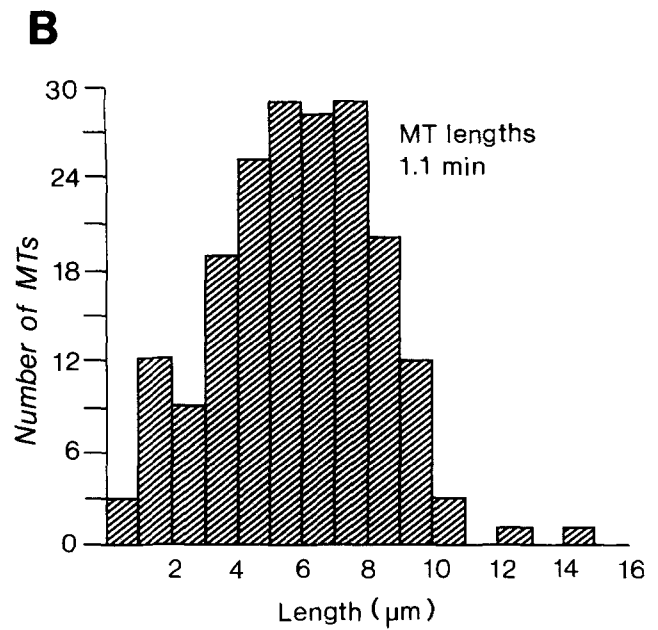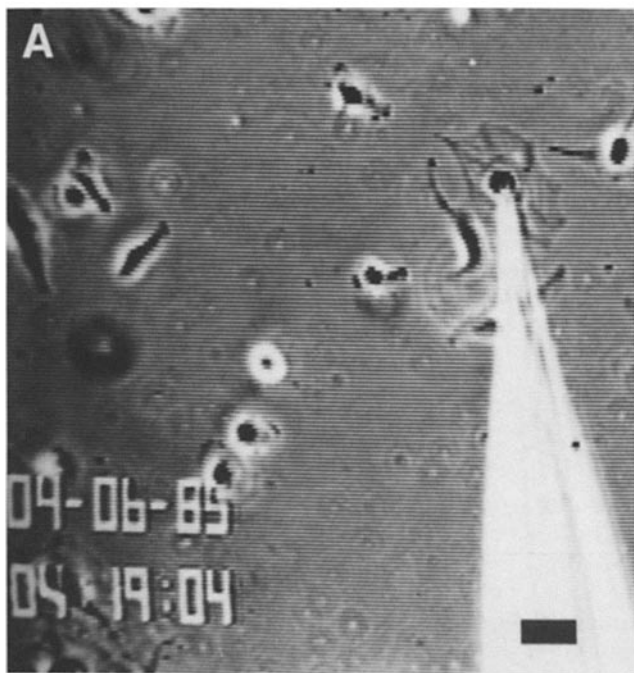
Figure 3. Microinjection and detection of biotin–tubulin. (*A*) Phase photovideomicrograph of a cell being injected with 5.0 mg/ml of biotin–tubulin. Bar, 50 μm. (*B*) Histogram of biotin-labeled microtubule segment lengths from *D* (mean = 5.9; SD = 2.4). (*C*) Fluorescein anti-tubulin immunofluorescence micrograph showing total microtubule network. The arrow points to the centrosome in both *C* and *D*. (*D*) Rhodamine anti-biotin immunofluorescence micrograph showing biotin-labeled microtubule segments. The cell was fixed 66 s after injection. Bar, 10 μm.
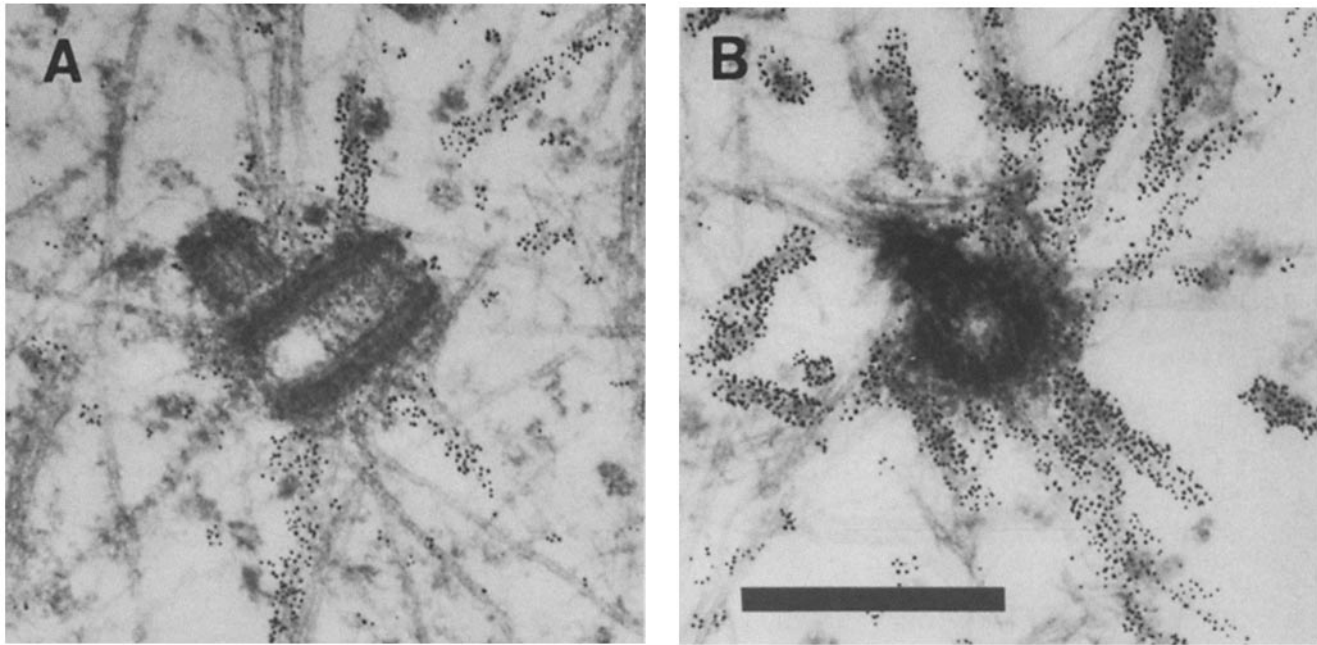
Figure 4. Thin-section electron micrographs of longitudinal and cross sections of centrioles. Cells were injected with biotin–tubulin and then stained with rabbit anti-biotin and colloidal gold goat anti-rabbit. A and B show unlabeled microtubules along with newly nucleated biotin-labeled microtubule segments. Bar, 0.5 μm.

cells are viewed by electron microscopy (Fig. 4), it becomes clear that labeled biotin segments are directly attached to osmiphyllic material surrounding the centrosome. In the same section, unlabeled microtubules also can be seen emanating from the centrosome. We have not seen any microtubules labeled proximally to the centrosome and unlabeled distally. Thus, within the limitations of the resolution of the experiment, there is no proximal addition of tubulin subunits onto pre-existing microtubules attached to the centrosome, although there is continuous new nucleation.

The Rate of Microtubule Elongation In Vivo

Since modification with biotin does not appear to perturb the assembly kinetics at low molar ratios of biotin–tubulin to unlabeled tubulin in vitro (Table I), we believed that it should be possible to obtain accurate measurements of the rate of microtubule elongation in vivo. To determine the rate of elongation we measured the average length of biotin segments at various times after injection. The exact time between injection and fixation was calculated from the video tape recording made during the procedure. Fig. 3D shows the video recording of the phase-contrast image of a cell being injected with 5 mg/ml biotinylated tubulin. Fig. 3C shows the same cell stained with anti-tubulin and Fig. 3D shows the anti-biotin labeling of the microtubule ends in the same cell permeabilized and fixed 66 s after injection. Fig. 3B gives a histogram of segment lengths for the cell pictured in 3D. Similar images were obtained for 64 cells representing over 10,000 segment lengths. At short times (<3 min), most of the segments represent elongation of existing microtubules rather than new nucleation off the centrosome. Fig. 5C shows a plot of the mean segment length vesus time for cells injected under the condition shown in Fig. 3. Although the standard error of the mean (SEM) for each time point varied from 0.05 to 0.54, the SEM for the slope (calculated from a weighted least

squares line constrained to pass through the origin) using the mean values was only 0.04.

An important consideration in interpreting such quantitative results is the question of whether the injection of biotinylated tubulin perturbs the cell's steady state. To address this we have varied the concentration tubulin injected and measured the rate of assembly. Extrapolation of the rate to zero molar ratio of biotin–tubulin to cellular tubulin should give the true in vivo rate of subunit incorporation. For this analysis, only short incubation times were used (<3 min) because labeled microtubules become very dense with time and difficult to measure. Even at the shortest times (20 s), microtubule segments are labeled in all regions of the cell, suggesting that the biotin–tubulin has been able to diffuse throughout the cell from the site of injection. Fig. 5, A–D, shows data collected from 64 cells injected for various times with tubulin concentrations of 0.5, 1, 5, and 10 mg/ml. The respective rates of microtubule elongation are 3.5, 3.6, 3.9, and 3.7 μm/min (see Table II).

At the highest concentration injected, we estimated that the total tubulin pool was increased by ~50% and at the lowest concentration, the total tubulin pool increased by only 2.5% (see Discussion). We were surprised that at the highest concentration no effect was observed on the rate of assembly when the free tubulin pool should have been significantly augmented (perhaps doubled). Since we know that high molar ratios of biotin–tubulin to tubulin are inhibitory in vitro, we surmised that at high concentrations the inhibition of assembly by biotin–tubulin may be offsetting the increased concentration of tubulin. To test this we injected two mixtures of biotin-labeled tubulin and unlabeled tubulin at two different total tubulin concentrations. As shown in Table II, when 10 mg/ml of tubulin was injected containing 9 mg/ml of unlabeled tubulin and 1 mg/ml of biotin–tubulin, the rate of assembly was greater than when pure biotin–tubulin (10 mg/

ml) was injected (7.7 μm/min compared to 3.7 μm/min). The rate of microtubule assembly in cells injected with 4 mg/ml pure tubulin and 1 mg/ml biotin–tubulin was 7.0 μm/min compared with 3.9 μm/min for 5 mg/ml biotin–tubulin. Thus an increase in intracellular free tubulin concentration produced by injection of unmodified tubulin can cause an increase in the elongation rate. The fact that at between 5 and 10 mg/ml the growth rate increases only slightly is interesting and may reflect other rate-limiting steps. From these results we conclude that injection of either 0.5 or 1.0 mg/ml biotinylated tubulin (which should increase the tubulin pool by only 2.5-5%) should not significantly perturb microtubule dynamics in vivo.

Turnover of Microtubules

5 min after injection, many of the labeled microtubules seem to have uniformly incorporated biotin–tubulin along their entire length. These labeled microtubules co-exist with unlabeled microtubules, which appear completely unlabeled except for their ends. With time there is a progressive replacement of unlabeled microtubules with labeled microtubules. This is illustrated in Fig. 6. Fig. 6A shows the anti-tubulin staining of a cell fixed 5 min after injection and Fig. 6B shows the anti-biotin staining of the same cell. Microtubules are seen to run from the centrosomal region to the periphery, but many microtubules have not incorporated label. By 15 min (Fig. 6, C and D), the majority of microtubules are completely labeled but again totally unlabeled microtubules remain. Our crude estimate is that by 15 min, 80 ± 10% of the microtubules are completely labeled, corresponding to a half-life of 5 to 10 min.

Evidence for a Quasi-stable Class of Microtubules

A complete analysis of incorporation of biotin–tubulin over long periods of incubation is difficult because of the ambiguity of tracing biotin segments among unlabeled segments as the former grow longer and become more numerous. It is clear, however, that even by 2 h a significant number of unlabeled microtubules still remain (Fig. 7). We have even seen a few unlabeled microtubules at 6 h. This quasi-stable class is not completely stable since by 12 h we can find no unlabeled segments (Fig. 8, A and B, and insets). By 24 h, some cells which have been injected undergo division to give daughter cells with completely labeled cytoskeletons (Fig. 9). This suggests that the labeled tubulin does not inhibit the formation of a functional mitotic spindle and that there is not extensive degradation of the modified tubulin.

Discussion

The object of this study is to determine where and at what rate tubulin subunits are incorporated into microtubules in interphase cells. The validity of this approach depends on how accurately biotin–tubulin reflects the behavior of native tubulin subunits. In this paper, we have tested the properties of biotin–tubulin both in vitro and in vivo. Tubulin modified by 2 to 3 biotins will assemble into microtubules in vitro (Mitchison and Kirschner, 1985a) and when it is used to study the sites of subunit addition at steady state in vitro, it adds only to the ends of microtubules (Kristofferson et al., 1986). Though modification with biotin diminishes somewhat the rate of assembly and the overall stability of the polymer, the extent of these effects is diminished when biotin–tubulin is used as a tracer at low molar ratios to native tubulin. For example, at a molar ratio of 1:19 the kinetic parameters of assembly differ only slightly from that of pure tubulin (Table I). In all in vitro experiments where biotin–tubulin is mixed with unmodified tubulin, the biotin–tubulin is found evenly distributed throughout the microtubules (Kristofferson et al., 1986).

When biotin–tubulin is injected into cells, short segments of incorporation are seen. As shown, for example, in Fig. 1,
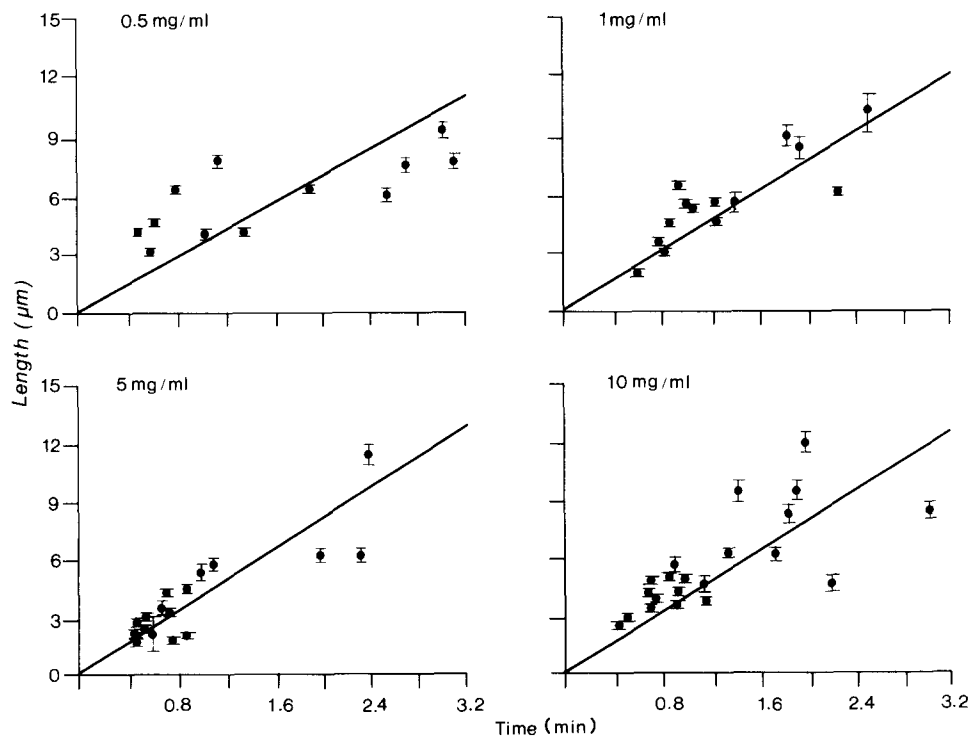

Figure 5. Mean biotin-labeled segment lengths vs. time of incubation after injection with biotin–tubulin. Biotin segment lengths were measured in injected cells at the indicated time points. Four different biotin–tubulin concentrations were injected as indicated in the figures. Each point represents the average segment length in a given cell. The error bars are ±1 SEM. The line is a weighted linear least square fit constrained to intersect the origin. The slopes in order of increasing concentrations are 3.5, 3.6, 3.9, 3.7 μm/min, respectively.
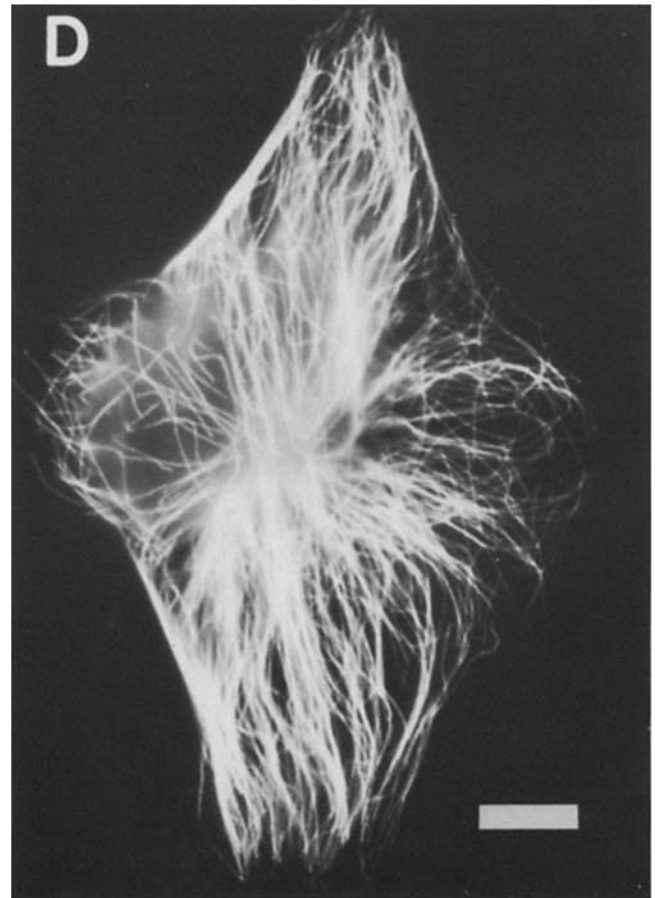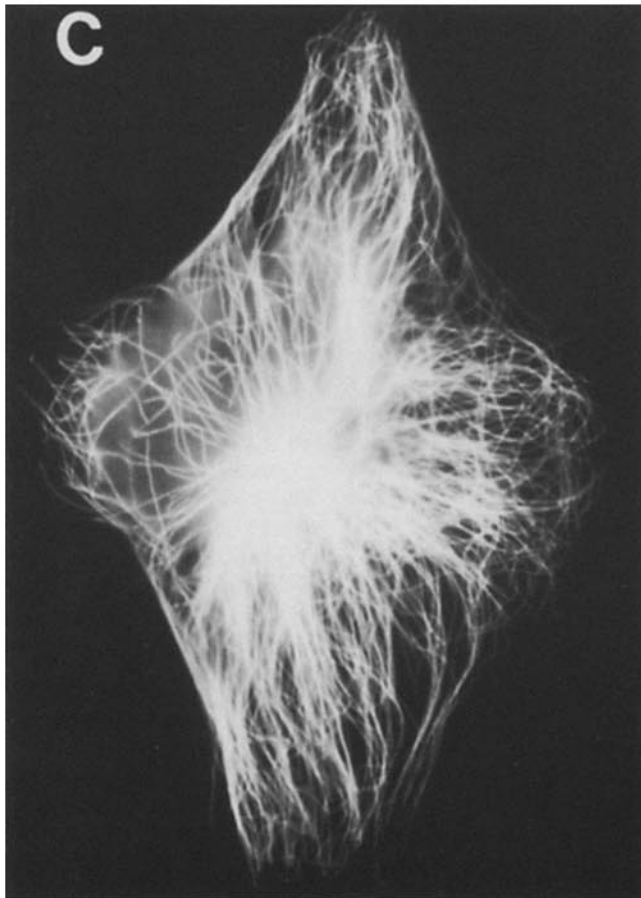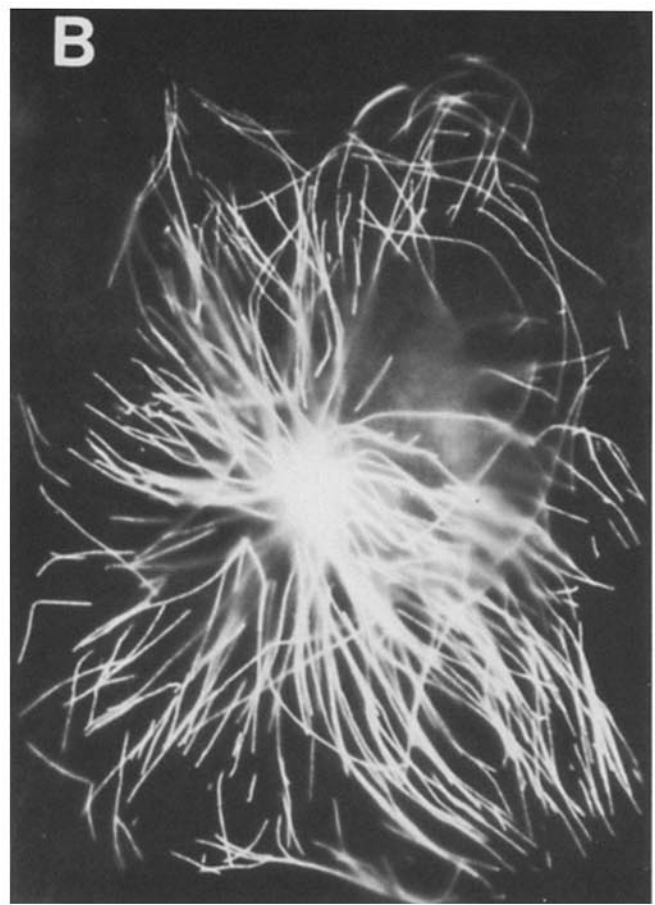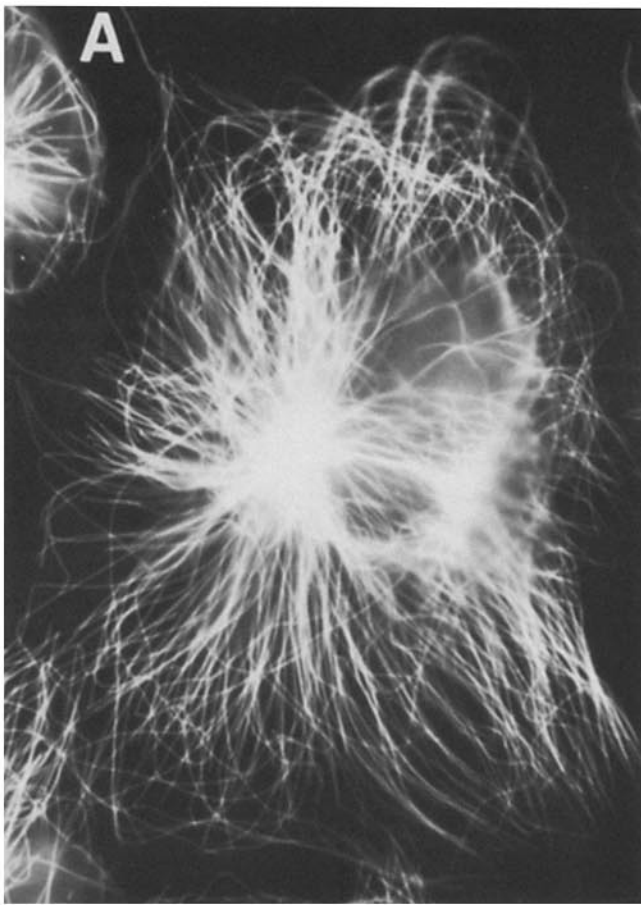
Figure 6. Double-label immunofluorescence of injected cells showing progressive replacement of unlabeled microtubules with labeled microtubules. (*A*) Fluorescein anti-tubulin staining showing total microtubule network in a cell injected 5 min before fixation. (*B*) Rhodamine anti-biotin staining of cell in *A* showing microtubule growth after a 5-min incubation after injection. (*C*) Fluorescein anti-tubulin staining of cell fixed 15 min after injection of biotin–tubulin. (*D*) Rhodamine anti-biotin staining of cell seen in *C* showing microtubule growth during a 15-min incubation with biotin–tubulin. Bar, 10 μm.
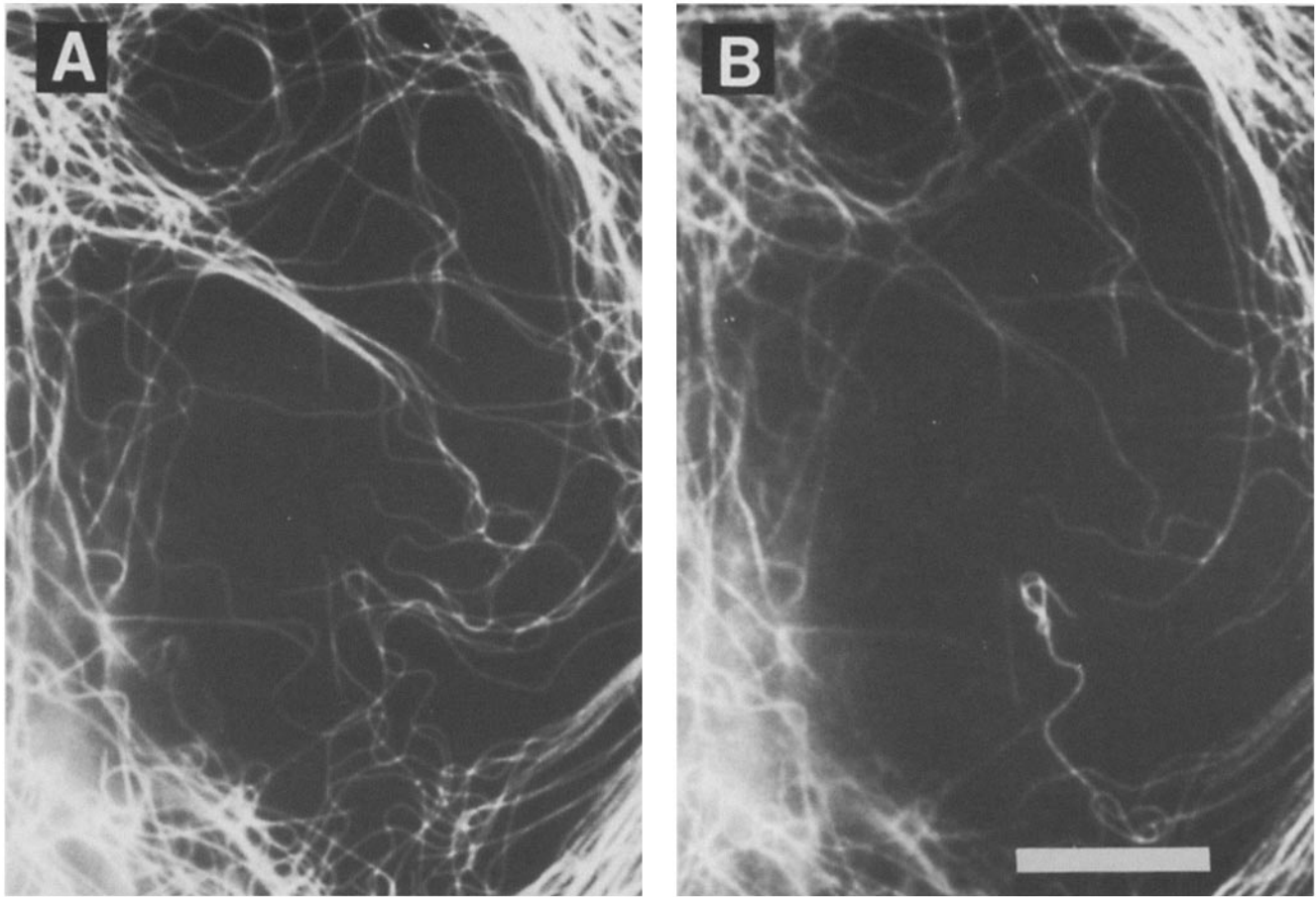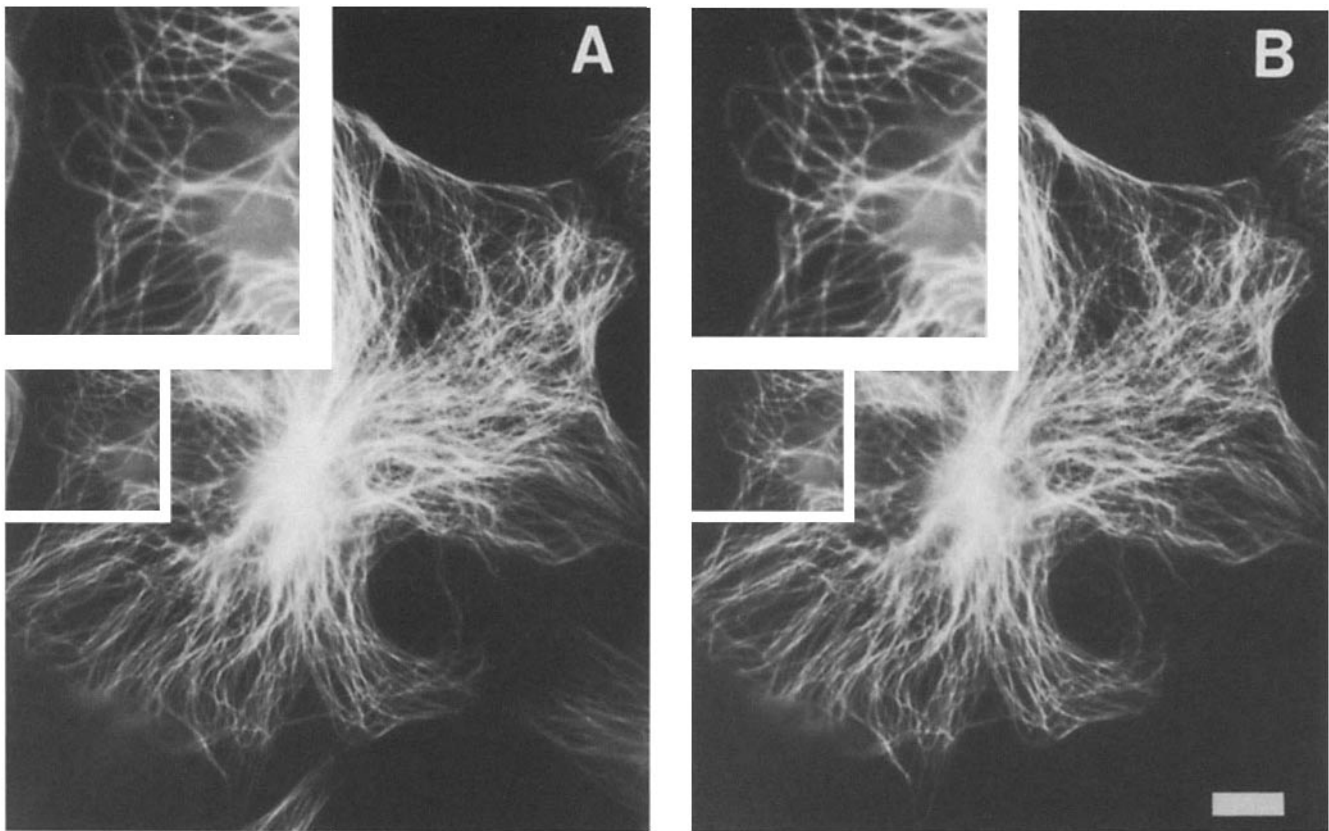
Figure 7. Double-label immunofluorescence revealing the existence of quasi-stable microtubules 2 h after injection of biotin–tubulin (10 mg/ml). (*A*) Fluorescein anti-tubulin staining of microtubule network in BSC1 fibroblast. (*B*) Rhodamine anti-biotin staining of the same cell area. Microtubules in *A*, but not in *B* represent microtubules which have not exchanged subunits with the free tubulin subunit pool over a 2-h incubation with biotin–tubulin. This area of the cell is particularly rich in stable microtubules.

most microtubule ends identified by total tubulin fluorescence have a labeled segment. In the interior of the cell where it is difficult to identify microtubule ends, a similar pattern of segmental incorporation is observed as seen on the periphery. This suggests that microtubule ends are dispersed throughout the cell and incorporate tubulin. However, we cannot assert that every labeled segment is associated with a microtubule end, and it remains possible that some of the segments represent spontaneous assembly. On the light microscope level there is no evidence for incorporation of subunits along the microtubule wall in agreement with the results of Soltys and Borisy (1985). A more rigorous examination by electron microscopy supports the contention that a clean junction always exists between labeled and unlabeled segments. The existence of a few deposits of colloidal gold not associated with microtubules is most likely due to the presence of microtubules above or below the plane of the section.

Whether the pattern of subunit exchange reflects the in vivo condition or merely represents spontaneous polymerization or additional assembly from the ends of microtubules driven by the increased tubulin concentration depends on whether the injected tubulin has perturbed the steady state. Although one might argue that at the lowest concentration of injected biotin–tubulin the overall tubulin concentration is changed very little, in fact little is known about the actual pool of free subunits. In our first experiments, we injected

biotin–tubulin at 10 mg/ml, which we roughly estimated would increase the total tubulin in the cell by 50% and the free tubulin pool by 100%. For this estimate we assume that the injection volume is 10% of the cell volume, that the total concentration of tubulin is 2 mg/ml (Hiller and Weber, 1978), and that 50% of tubulin is polymerized (Hiller and Weber, 1978; Soltys and Borisy, 1985; Caron et al., 1985). However, in later experiments with improved detection methods, we could detect biotin–tubulin when injected at a concentration as low as 0.5 mg/ml. This concentration should increase the total tubulin concentration by only 2.5%. To test whether the injected tubulin perturbs the steady state, we calculated an approximate rate of polymerization at various concentrations of injected tubulin by measuring the average segment length at various times after injection (Table II). The reproducibility of the concentration produced in an injected cell is probably very poor because the volume injected and the cell volume are not known precisely. However, over a 20-fold concentration range we were confident in having extensively varied the internal concentration and this was reflected in the expected diminution of the biotin–tubulin signal with decreasing concentrations of injected biotin–tubulin. As shown in Fig. 5 and Table II, the rate of subunit incorporation, ($\approx$3.6 μm/min) was nearly the same at all concentrations suggesting that no major perturbation had occurred. It was surprising that no augmentation of the rate had occurred at the highest concen-

Figure 8. Double-label immunofluorescence of a cell injected 12 h before fixation demonstrating complete turnover of the microtubule cytoskeleton. (*A*) Fluorescein anti-tubulin staining of the microtubule network. (*B*) Rhodamine anti-biotin staining. Insets are a twofold magnification of the outlined area situated close to the nucleus. Inspection reveals a 1:1 correspondence of labeled and unlabeled microtubules. Note: cell in upper right was also injected. Bar, 10 μm.
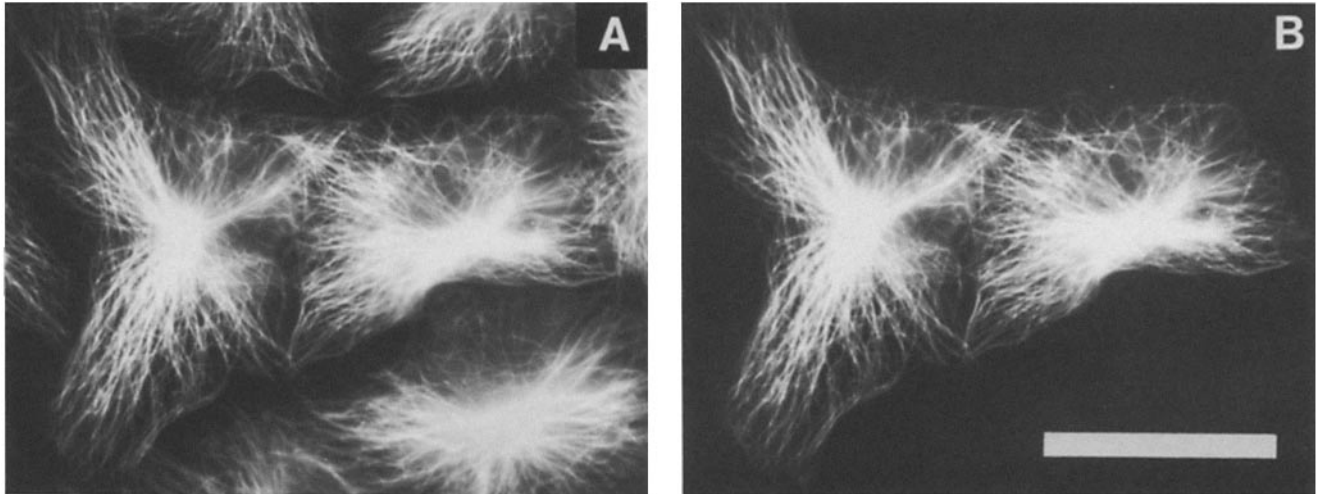
Figure 9. Double-label immunofluorescence of two daughter BSC1 cells fixed 24 h after injection of the mother cell. This demonstrates that biotin–tubulin does not prevent transit through the cell cycle. (*A*) Fluorescein anti-tubulin staining of the microtubule network. (*B*) Rhodamine anti-biotin staining of the same two daughter cells. Bar, 40 μm.

tration, 10 mg/ml, and we could show that this was probably due to offsetting effects of increased tubulin monomer level and inhibition of assembly at the high molar ratio of biotin–tubulin. At low concentrations (0.5 and 1 mg/ml) when we pool all of the elongation rate data, we find an overall growth rate of 3.6 μm/min which corresponds to ~100 subunits/s, a rate that is about two times faster than that for pure tubulin

at steady state in vitro (Mitchison and Kirschner, 1984b). Based on the above experiments we conclude that biotin–tubulin can act as a tracer in these studies and that the measured incorporation rates should reflect in vivo microtubule dynamics.

It is interesting to consider the significance of a rate of growth of 3.6 μm/min in these cells. Since the average distance

from the nucleus to the cell periphery is 20 μm, it would take ~5 min for a microtubule to grow from the centrosome to the cell periphery. In fact, by 5 min, many completely labeled microtubules can be seen extending from the centrosome to the cell periphery. Accompanying microtubule elongation is new nucleation from the centrosome. This new assembly at the centrosome is confirmed by electron microscopy and colloidal gold staining. Since there is very rapid growth of most microtubules and new nucleation off the centrosome, there must also be a concomitant depolymerization of other microtubules or else the cell would quickly exhaust its tubulin pool. In fact, at the observed rate of subunit incorporation, the entire microtubule array must turnover in <15 min and this is, in fact, what is observed for the majority of microtubules in the cell (see Fig. 6, *C* and *D*).

It is important to note that rapid exchange in a given microtubule occurs to completion in a short time for a majority of microtubules. Fully labeled microtubules seem to arise by new growth from the centrosome. Using the present methods of analysis, however, we could not evaluate quantitatively the change in the number of labeled microtubules at the centrosome because light microscopy cannot resolve the microtubules in the thick region of the cell and thin sectioning does not easily give a complete quantitative picture. Nevertheless, the clear evidence of new nucleation plus the increase in the numbers of new fully labeled microtubules with time suggest that the microtubule population is rapidly being replaced by new microtubule growth from the centrosome which must, at steady state, be balanced by a compensatory loss of other microtubules.

The measurements of microtubule growth rate in vivo and the pattern of subunit incorporation can be used to evaluate the applicability of various models of microtubule behavior inferred from in vitro experiments. Microtubules are clearly not in simple equilibrium with their subunits at the end of the microtubules because such dynamics would lead to slow diffusional exchange at the ends. Neither is exchange of subunits along the microtubule walls of much importance. Though this could have explained the rapid and complete exchange, it clearly does not occur since completely unlabeled polymers co-exist with heavily labeled ones in the same EM section (Fig. 2) and a sharp demarcation between labeled and unlabeled segments always exists in the same microtubule. Treadmilling could in principal produce more rapid incorporation than diffusional exchange. However, even if treadmilling occurs, it is unlikely to be the mechanism for observed

dynamics. Treadmilling would predict that subunits would invade existing polymer from either end but should operate similarly on all microtubules. This is not what is observed. Microtubules are replaced one by one in a seemingly stochastic manner. In addition, the rate of subunit incorporation and polymer turnover is orders of magnitude faster than the fastest observed rates of treadmilling (rate of growth in vivo is 100 subunits/s compared to in vitro treadmilling values of 5 to 25) (Cote and Borisy, 1981; Margolis and Wilson, 1978). In summary, the major means of subunit turnover in the cell is the replacement one by one of microtubules nucleated at the centrosome with new microtubules.

Recent studies of microtubule dynamics in vitro provide at present the most useful model for understanding these in vivo properties (Hill and Carlier, 1983; Kristofferson et al., 1986; Mitchison and Kirschner, 1984b; Chen and Hill, 1983). Microtubules have been demonstrated to exist in growing and shrinking phases which interconvert infrequently, a property thought to be related to the presence or absence of GTP-liganded subunits at the end of the microtubule. Thus, in vitro, a given microtubule grows until it shifts into the shrinking phase with some probability inversely related to its rate of growth. This property, called dynamic instability, makes even a steady-state population very dynamic. When centrosomes are present, they are a permanent source of microtubule nucleation. The microtubules that are produced grow for a while, shift to the depolymerizing phase, and are replaced by new microtubules. A similar pattern of microtubule replacement seems to be occurring in the interphase fibroblast cell, as described here and therefore dynamic instability seems consistent with the observed behavior in vivo.

Although most microtubules in vivo appear to be very unstable, some apparently do not participate in the rapid subunit exchange. As shown in Fig. 7, microtubules remain which do not exchange subunits for 2 h or more, although they do turnover at a slower rate and have fully exchanged by 12 h. If the half time of exchange for the dynamic microtubules is 5–10 min, we would expect <1% to remain after 2 h. In fact, ≈10% of the population has not exchanged by 2 h. We do not know if these stable microtubules represent a single class or a continuum of classes of increased stability. We cannot as yet ascribe any functional or structural significance to these stable microtubules, nor have we been able to find a common origin such as a particular place on the centrosome. However, given the diverse functions of microtubules in cells, for example, motility, transport, and cellular organization,

Table II. Effect of Biotin–Tubulin on Microtubule Elongation Rates In Vivo

Concentration injected	Molar ratio of injected tubulin (biotin–tubulin/tubulin)	Estimated % increase in free tubulin concentration*	Estimated molar ratio produced in vivo[‡] (biotin–tubulin/tubulin)	Microtubule elongation rate (μm/min)[§]
		%		
0.5 mg/ml	1:0	5	1:20	3.5 ± 0.03
1.0 mg/ml	1:0	10	1:10	3.6 ± 0.03
5.0 mg/ml	1:0	50	1:2	3.9 ± 0.03
10.0 mg/ml	1:0	100	1:1	3.7 ± 0.03
5.0 mg/ml	1:4	50	1:14	7.0 ± 0.09
10.0 mg/ml	1:9	100	1:19	7.9 ± 0.08

* The intracellular free tubulin concentration is assumed to be 1 mg/ml (Hiller and Weber, 1978), and we assume that 1/10 of a cell volume is injected, i.e. when 1 mg/ml biotin–tubulin is injected, the final tubulin concentration is increased by 10%.
[‡] Calculated assuming the same parameters as *.
[§] The indicated errors are ±1 SEM ($s/\sqrt{n}$).

this kinetic differentiation is likely to reflect functional distinctions. Two generally plausible mechanisms could account for these stable microtubules. First, microtubules could be "capped" both at the centrosome and at the "free" or "plus" end by as yet uncharacterized capping factors. Capping at both ends would remove these microtubules from the overall equilibrium. Alternatively, microtubules could be differentiated along the entire length by microtubule-associated proteins or by posttranslational modification of tubulin (Thompson et al., 1984; Gundersen et al., 1984). These mechanisms are not mutually exclusive since an initial end-dependent stabilization could allow a time-dependent modification along the entire microtubule to take place (Mitchison and Kirschner, 1985b).

The dynamic studies presented here are consistent with the fluorescent tubulin incorporation results of Saxton et al. (1984). They observed a half-time of incorporation of 20 min, where we observed 10 min. They also found incomplete recovery of the fluorescent signal which we would now ascribe to a minority population of stable microtubules. They observed no overall geometrical pattern to the recovery which suggested no wave of treadmilling or regrowth was occurring and might have suggested exchange of subunits along the polymer wall. This, however, can be explained more easily by the stochastic nature of microtubule regrowth from both pre-existing microtubule ends and continuous renucleation off the centrosome. At the level of resolution of the photobleaching recovery method, the random growth of single microtubules through the photobleached spot would not have been resolved.

Together with the essentially bulk incorporation and photobleaching studies of Salmon et al. (1984a, b) and the labeling studies of Soltys and Borisy (1985), the kinetic results presented here redefine the steady state of microtubules in fibroblast cells. The static image from immunofluorescence is seen to be merely a snapshot of dynamic microtubule populations, where centrosomes continuously nucleate microtubules that disappear in a constant flux. We have also found evidence for the existence of quasi-stable microtubules in the same cell as dynamic ones, a finding which was inferred from earlier pharmacological studies (Behnke and Forer, 1967). This differential stability gives the cell a new parameter to vary for microtubule function.

References

Albrecht-Buehler, G. 1976. Filopodia of spreading 3T3 cells: do they have a substrate exploring function? J. Cell Biol. 69:275-286.

Behnke, P., and A. Forer. 1967. Evidence for four classes of microtubules in individual cells. J. Cell Sci. 2:169-192.

Bradford, M. M. 1976. A rapid and sensitive method for the quantitation of microgram quantities of protein utilizing the principle of protein-dye binding. Anal. Biochem. 72:248-254.

Bray, D. 1973. Branching patterns of individual sympathetic neurons in culture. J. Cell Biol. 56:701-712.

Caron, J. M., A. L. Jones, and M. W. Kirschner. 1985. Autoregulation of tubulin synthesis in hepatocytes and fibroblasts. J. Cell Biol. 101:1763-1772.

Chen, Y.-D., and T. L. Hill. 1983. Use of Monte Carlo calculations in the study of microtubule subunit kinetics. Proc. Natl. Acad. Sci. USA. 80:7520-7523.

Cote, R. H., and G. G. Borisy. 1981. Head to tail polymerization of microtubules in vitro. J. Mol. Biol. 150:577-602.

De Brabander, M., G. Geuens, R. Nuydens, R. Willebrords, and J. De Mey. 1981. Microtubule assembly in living cells after release from nocodazole block: the effects of metabolic inhibitors, taxol and pH. Cell Biol. Int. Rep. 5:913-920.

Drubin, D., S. Kobayashi, and M. Kirschner. 1985. Association of tau protein with microtubules in living cells. Ann. NY Acad Sci. In press.

Graessmann, A., M. Graessmann, and C. Mueller. 1980. Microinjection of early SV40 DNA fragments and T antigen. Methods Enzymol. 65:816-825.

Graessmann, M., and A. Graessmann. 1976. "Early" simian-virus-40 specific RNA contains information for tumor antigen formation and chromatin replication. Proc. Natl. Acad. Sci. USA. 72:266-370.

Gundersen, G. G., M. H. Kalnoski, and J. C. Bulinski. 1984. Distinct populations of microtubules: tyrosinated and nontyrosinated alpha tubulin are distributed differently in vivo. Cell. 38:779-789.

Hill, T. L., and M. W. Kirschner. 1982. Bioenergetics and kinetics of microtubule and actin filament assembly-disassembly. Int. Rev. Cytol. 84:185-234.

Hill, T. L., and M. F. Carlier. 1983. Steady state theory of the interference of GTP hydrolysis in the mechanism of microtubule assembly. Proc. Natl. Acad. Sci. USA. 80:7234-7238.

Hiller, G., and K. Weber. 1978. Radioimmunoassay for tubulin: a quantitative comparison of the tubulin content of different established tissue culture cells and tissues. Cell. 147:795-804.

Inoué, S., and H. Sato. 1967. Cell motility by labile association of molecules. J. Gen. Physiol. 50(Suppl.):259.

Inoué, S. 1982. The role of self-assembly in the generation of biologic form. In Developmental Order: Its Origin and Regulation. S. Subtelny and P. Green, editors. Alan R. Liss, Inc., New York. 35-77.

Inoué, S., and H. Ritter. 1975. Molecules and Cell Movement. S. Inoué and R. Stephens, editors. Raven Press, New York. 3-10.

Karsenti, E., S. Kobayashi, T. Mitchison, and M. Kirschner. 1984. Role of the centrosome in organizing the interphase microtubule array: properties of cytoplasts containing or lacking centrosomes. J. Cell Biol. 98:1763-1776.

Kirschner, M. 1980. Implications of treadmilling for the stability and polarity of actin and tubulin polymers in vivo. J. Cell Biol. 86:330-334.

Kristofferson, D., T. Mitchison, and M. Kirschner. 1986. Direct observation of steady-state microtubule dynamics. J. Cell Biol. 102:1007-1019.

Margolis, R. L., and L. Wilson. 1978. Opposite end assembly and disassembly of microtubules at steady state in vitro. Cell. 13:1-8.

Mitchison, T., and M. Kirschner. 1984a. Microtubule assembly nucleated by isolated centrosomes. Nature (Lond.). 312:232-237.

Mitchison, T., and M. Kirschner. 1984b. Dynamic instability of microtubule growth. Nature (Lond.). 312:237-242.

Mitchison, T. J., and M. W. Kirschner. 1985a. Properties of the kinetochore in vitro. I. Microtubule nucleation and tubulin binding. J. Cell Biol. 101:755-765.

Mitchison, T., and M. Kirschner. 1985b. Molecular Biology of the Cytoskeleton. Cold Spring Harbor Press, New York. In press.

Oosawa, F., and S. Asakura. 1975. Thermodynamics of the Polymerization of Protein. Academic Press, Inc., New York. 204 pp.

Salmon, E. D., W. M. Saxton, R. J. Leslie, M. L. Karos, and J. R. McIntosh. 1984a. Diffusion coefficient of fluorescein-labeled tubulin in the cytoplasm of embryonic cells of a sea urchin video image analysis of the fluorescence redistribution after photobleaching. J. Cell Biol. 99:2157-2164.

Salmon, E. D., R. J. Leslie, W. M. Saxton, M. L. Karow, and J. R. McIntosh. 1984b. Spindle microtubule dynamics in sea urchin embryos: analysis using a fluorescein-labeled tubulin and measurements of fluorescent redistribution after laser photobleaching. J. Cell Biol. 99:2165-2174.

Saxton, W. M., D. L. Stemple, R. J. Leslie, E. D. Salmon, M. Zavortink, and J. R. McIntosh. 1984. Tubulin dynamics in cultured mammalian cells. J. Cell Biol. 99:2175-2186.

Soltys, B. J., and G. G. Borisy. 1985. Polymerization of tubulin in vivo: direct evidence for assembly onto microtubule ends and from centrosomes. J. Cell Biol. 100:1682-1689.

Thompson, W. C., D. J. Asai, and D. H. Carney. 1984. Heterogeneity among microtubules of the cytoplasmic microtubule complex detected by a monoclonal antibody to alpha tubulin. J. Cell Biol. 98:1017-1025.

Weingarten, M. D., A. H. Lockwood, S. Hwo, and M. W. Kirschner. 1975. A protein factor essential for microtubule assembly. Proc. Natl. Acad. Sci. USA. 72:1858-1862.